

Chapter 11

Modelling of Coupled Thermo–elastoplastic–hydraulic Response of Clays Subjected to Nuclear Waste Heat

T. Hueckel, M. Borsetto, and A. Peano

11.1 INTRODUCTION

One of the hypotheses for disposal of nuclear waste of long-lived radioactivity is the construction of repositories in deep clay formations. Principal candidate rocks in Italy are largely diffused pliocenic clays.

The prominent feature of clay as a nuclear waste storage medium is its low permeability ranging from 10^{-8} to 10^{-12} m/sec. It offers an effective barrier to far-field natural water migration and possible transport of radionuclides towards the human environment. However, such a situation may be disturbed by the thermal effect of radioactive decay. In its consequence, heat transfer occurs through the geological formation, associated with development of pore water pressure and its dissipation via a water seepage. Heating and seepage involve effective stress and strain changes in clay skeleton. Specifically, the decay heat of the waste may significantly affect the water–soil equilibrium in the very vicinity of the repository and give rise to undesired high pore water pressure build-up around canisters and/or water flow off and towards the repository. Such phenomena may have technological implications, mostly concerning engineering of repository construction and emplacement techniques and therefore deserve a particular attention.

Clay is a multiphase medium and thus develops complex stress and strain microstructural fields in response to heating. At depths suitable for nuclear waste repositories, clays are fully saturated with water under a high hydrostatic pressure. For this reason even at temperatures around 150°C , no water vaporization may be expected as seen from a one-year test under 0.6 MPa of confinement stress at 160°C [1]. Therefore, no gaseous fraction is

taken into account in what follows. Clay is considered thus as two-phase medium comprised of a solid mineral phase and water.

Thermal changes in the water-solid interaction, affect clay behaviour on three levels, i.e. on the level of the boundary value problem, on the level of phenomenological material properties and finally on the microstructural level. In phenomenological experiments clay exhibits both non-linearity and irreversibility of mechanical and thermal deformational and hydraulic behaviour.

In this paper, some of such macroscopic experimental results are presented concerning mostly the thermomechanical effects in clays. A microstructural qualitative interpretation especially of the thermal shrinkage of clay observed in some circumstances is given afterwards. Then a macroscopic model is developed. In the model the aforementioned non-linear effects are taken into account. For the mechanical part a Cam-clay type model is adopted and generalized to thermoplastic effects. On this basis prospective scenarios of the very near field repository performance are discussed, resulting from hydraulic-thermo-mechanical coupling on the boundary value problem level. An example of a near field numerical analysis is given.

11.2 THERMO-MECHANICAL AND HYDRAULIC PROPERTIES OF CLAYS

11.2.1 General remarks

Italian pliocenic clay formations are sediments consisting of finest grains of soils and mineral products of rock degradation deposited under marine conditions. Due to subsequent geologic agents such as environmental condition, lithostatic pressures, cementation, etc, clays exhibit a particular complexity of microstructure. Its prominent feature is an interaction on the microstructural level of the solid and liquid phase, it is of the clay skeleton and water.

Unlike some other granular materials, clay cannot be separated into a solid and liquid phase under normal conditions. In fact, it is known, that water in clay may appear in four kinds of conditions, i.e. as pore water, loosely adsorbed water, firmly adsorbed water and structural one. These water phases interact with the solid fraction and react to thermal and hydraulic loads in different ways. In particular, water of the two first phases only, may migrate freely due to hydraulic gradients. Chemical bond energy between solid and water of other two categories may vary with temperature. It leads to exchanges of quantities of water between the phases due to heating. In consequence, known micromechanisms of generation of the elastic and plastic deformation of clay are affected by temperature. The above microstructural effects of skeleton-water interaction lead to a rather complex, non-linear behaviour of clay when observed in laboratory using macroscopic stress and strain measures. Simple intuition indicates that thermomechanical deformation of clay solid

depends on effective stress and temperature and on pore water-pressure rise induced by it. Pressure and flow of water depend, on the other hand, on permeability of clay, on water thermal expansion and porosity changes. Thermal properties, perhaps to the least extent, are function of stress or porosity variation.

In what follows, we shall examine deformational, hydraulic and thermal local behaviour relationships underlining their interdependences.

11.2.2 Thermo-mechanical effects in clay

It is well known that clay in athermal conditions *in situ* may be in the state of overconsolidation or of normal consolidation, depending on whether the actual vertical stress is respectively less than or equal to maximum vertical stress.

In the overconsolidation states clay deforms elastically. Yielding is reached only in the normal consolidation state. In thermal conditions the former hypothesis has been confirmed experimentally by performing a closed cycle composed of isothermal loading, constant pressure heating, isothermal unloading and cooling. On its complete closure the cycle produced virtually no irreversible strain [2].

The reversible volumetric strain is assumed to consist of solid grain compression due to water pressure, u , of effective stress induced deformation of clay skeleton and of thermal isotropic expansion both of grains themselves and of skeleton. The latter involves also possible structural and firmly adsorbed water changes. The reversible deviatoric strain are purely linear elastic. The thermoelastic relationship may be in general written as:

$$\epsilon^{el} = \frac{1}{3} \left\{ K(\Delta T) \ln \frac{\text{tr } \sigma'}{\text{tr } \sigma'_g} + \left[\alpha^* + \alpha_{st}(\Delta T, \ln \frac{\text{tr } \sigma'}{\text{tr } \sigma'_g}) \right] \Delta T + \bar{C}^* u \right\} \mathbf{m} + \frac{1}{2G} (\mathbf{S} - \mathbf{S}_g); \mathbf{m}^T = \{1, 1, 1, 0, 0, 0\} \quad (11.1)$$

where σ' is effective stress connected to pore water pressure u via effective stress relationship of Terzaghi: $\text{tr } \sigma = \text{tr } \sigma' + u$. $K = K(\Delta T)$ is known as effective elastic compression index and is supposed to depend on temperature. $\bar{C}^* = \text{const.}$ is the grain solid (mineral) compliance modulus. Also the coefficient of cubic thermal expansion of grain solid α^* , is assumed as constant; this is not the case of α_{st} , referred to as coefficient of thermal expansion of soil structure, after Campanella and Mitchell [3]. σ_g and \mathbf{S}_g are isotropic and deviatoric stresses existing in the clay mass in a geostatic state, i.e. prior to applying the engineering mechanical and thermal loading. G is the shear modulus considered as constant.

Thermal variations of the bulk modulus K and variations of α_{st} with temperature and with effective isotropic stress have been examined at ISMES in a high pressure, high temperature triaxial apparatus HITEP. The apparatus and experimental procedures are described elsewhere [4].

Results from a pressure-temperature cycle on an undisturbed Boom Clay sample from the 200 m depth Mol site are shown in Figure 11.1(a) and 11.1(b). As seen, thermal volumetric strains at constant effective pressure in the overconsolidation range take on negative values. Moreover, the thermal strains vary with effective mean stress and temperature. Such effects have been reported also for soft seabed clays, and for rocks under some conditions [3, 5]. Note a significant difference of the thermal curves. The difference in their performance, considered as elastic for the strong overconsolidation, may be attributed both to variation of $K = K(\Delta T)$ and of $\alpha_{st} = \alpha_{st}(\text{tr } \sigma')$ as may be deduced from Equation (11.1) by assuming α^* as constant and positive. If a hypothesis of derivability of Equation (11.1) from Gibbs free energy density function is experimentally verified some constraints must be imposed on the variations of K and α_{st} .

Several other experiments have been performed [4] on different clays and the following conclusions have been reached. The absence of plastic effects in the overconsolidation range has been confirmed by the closure of the strain cycle, discussed above. The influence of preconsolidation strain on thermal strain has been seen as negligible by varying the overconsolidation ratio at fixed value of effective stress at which heating was performed [4].

Thermal strain hysteresis loop upon heating and cooling at constant effective stress has the width less than 10% of the total strain [4]. Therefore, it can also be considered as a marginal effect unless heating cycle should repeat a number of times as to give rise to an accumulation of strain. Cyclic thermal loading is not however predicted by clay repository scenarios.

Let us consider now the behaviour in the range including normal consolidation and failure. In this range a substantial part of mechanically induced strain is irreversible. The same refers to the thermally induced strains. Irreversible strains are assumed to occur in the clay skeleton only. No plastic strain is expected in the grain mineral solid. Because of the history dependence of athermal purely plastic strains, a one-to-one stress-strain correspondence may be written between increments only. Also a thermomechanical strain may be defined only incrementally for given stress and temperature increments.

The plastic flow rule is affected by temperature what may be described as follows:

$$d\mathbf{e} = d\mathbf{e}' + d\mathbf{e}''; \quad d\mathbf{e}' = d\bar{\lambda}(dT, d\sigma') \frac{\partial g}{\partial \sigma'}(\sigma', \Delta T) \quad \left. \vphantom{d\mathbf{e} = d\mathbf{e}' + d\mathbf{e}''} \right\} \quad (11.2)$$

$$d\bar{\lambda} = 0 \quad \text{if } f < 0; \quad f = 0, d\bar{\lambda} < 0; \quad d\bar{\lambda} > 0 \quad \text{if } f = 0; \quad d\bar{\lambda} = 0 \quad \text{if } f > 0;$$

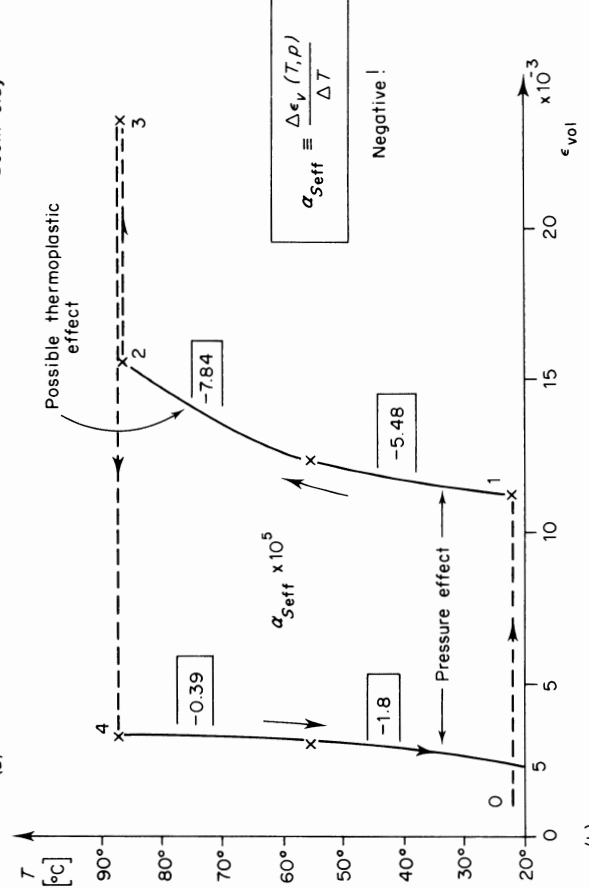
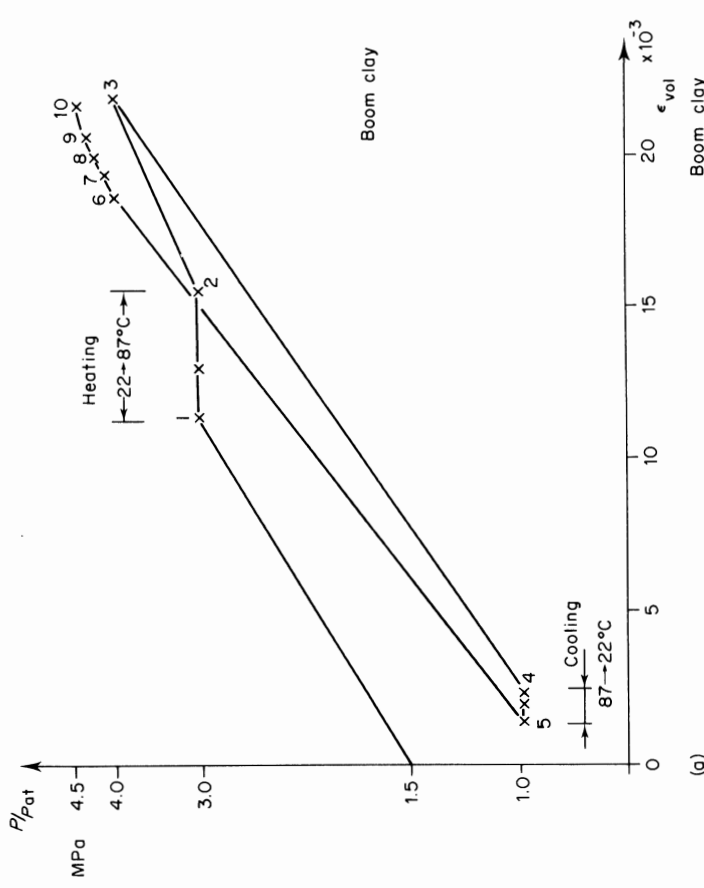


Figure 11.1 Volumetric strain in isotropic drained test in over-consolidated Boom clay. (a) Isotropic pressure-volumetric strain. (b) Temperature-volumetric strain.

Where $f = 0$ is the yield function and g is the plastic potential

$$f = f(\sigma', \Delta T); \quad g = g(\sigma', \Delta T) \quad (11.3)$$

The yield surface for clays intersects the isotropic stress axis both at the compression as well as at isotropic extension side. Its evolution is ruled by the variation of the plastic volumetric strain, dilative or contractive one, giving rise to respectively strain-softening or strain-hardening. A particularly simple ellipsoidal form of the yield surface known as modified Cam-Clay, which has been given a large experimental support in isothermal conditions, has been proposed by Roscoe and Burland [6]. Generalizing it to high temperature and high pressure conditions the following equation is proposed (the superscript T denotes transpose)

$$f = \left(1 - \frac{1}{3} \frac{\text{tr } \sigma'}{\alpha(\Delta T)} \right)^2 + \frac{\sqrt{3}}{\sqrt{2}} \frac{M(\Delta T)}{[gM(\Delta T)\alpha^m(\Delta T)]^2} (\mathbf{S}^T \mathbf{S}) - 1 = 0 \quad (11.4)$$

where $\alpha(\Delta T)$ is a major semiaxis of the ellipsoid, $M(\Delta T)$ is critical state functional coefficient, g is a function of the second and third stress deviator invariants, e.g. as proposed by Gudehus [7]. The stress deviator is defined in a standard way. The constant exponent m , $0 < m \leq 1$ describes the

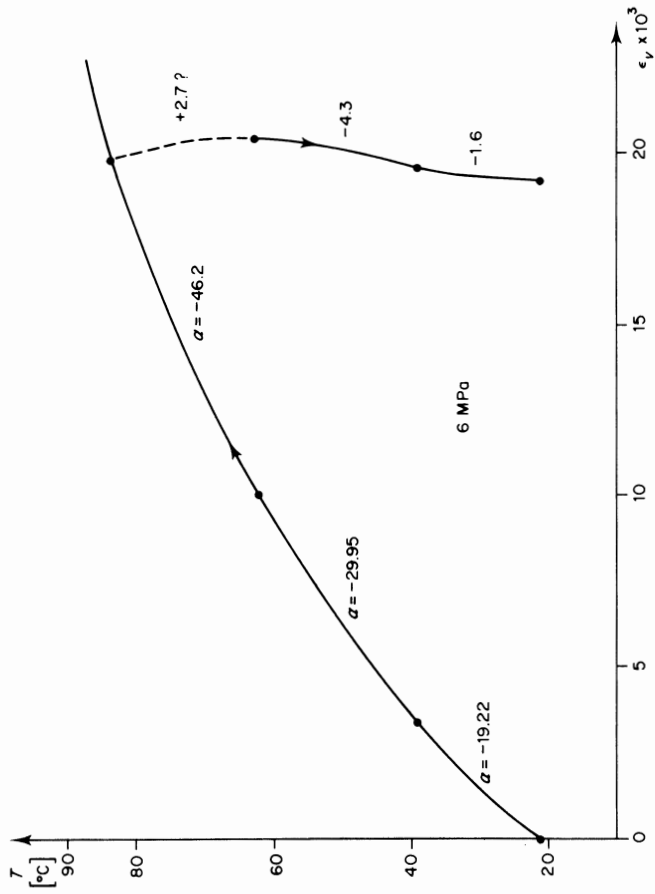


Figure 11.2 Thermal volumetric strain in Boom clay in normal consolidation state at constant isotropic pressure.

longitudinal curvature of a paraboloid critical state surface. The curvature of the critical state surface, which classically is a cone ($m = 1$), is due to high effective pressure. Clearly for $m \neq 1$ the physical meaning of the coefficient M is somewhat different.

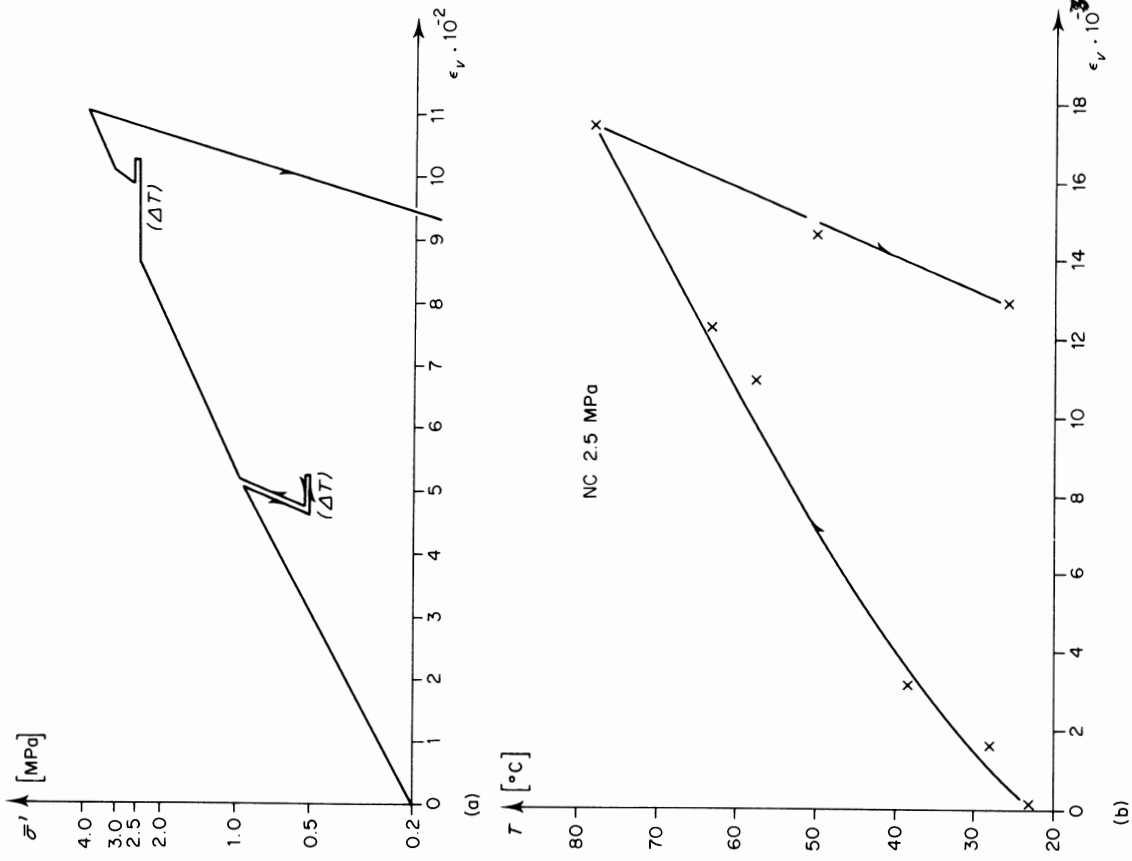


Figure 11.3 Volumetric strain in Pontida silty clay. (a) Against isotropic pressure. (b) Against temperature.

The plastic potential $g(\sigma', \Delta T)$ is in general different from the yield locus f , giving rise to the non-associativity of the plastic strain rate to the locus. A peculiarity of thermoplastic behaviour of clay, e.g. with respect to metals, stands in a variation of g with temperature in such a way that deviation of the thermoplastic strain rate from an athermal strain rate may vary as heating proceeds. This divergence seems to be pronounced in the softening range.

An example of thermal strain in normal consolidation state under drained conditions obtained from a heating/cooling test on Boom clay at constant isotropic stress is shown in Figure 11.2. Note that more than the two-thirds of the strain induced by heating remains after cooling. A similar result has been obtained on Pontida silty clay on which a complex stress-temperature program has been performed, Figure 11.3.

A derivation of a thermoplastic constitutive equation is given in Section 11.3.1.

11.2.3 Thermal water-solid coupling in the clay microstructure

The macroscopic experiments presented above indicate that heating may in some conditions cause shrinkage instead of expansion of the clay skeleton. Shrinkage is a well-known effect for much higher temperatures in brick technology. However, the mechanism of dehydration due to evaporation at free surface typical for ceramics in contact with air [8] is not likely to occur in immersion conditions at depth of interest here. Anyway, the principal microstructural mechanism of heating strain in immersion seems still to be the water phase exchange. Of the four phases of water in clay, i.e. structural, firmly adsorbed, loosely adsorbed and pore water [9], only the last two can leave the soil, when heated. It is most probable that shrinkage is caused by changes of configuration of the loosely adsorbed water due to reduction of its density and its partial transformation into pore water.

A generation of irreversible strains by heating confirms this hypothesis. In fact, the straining of clays under isotropic consolidation is usually attributed on microstructural level to the formation of contacts between mutually attracting grains of clay solid mineral [10]. The contacts are of two types, i.e. mineral-to-water-to-mineral (M-W-M) and mineral-to-mineral (M-M). In the latter contacts, grains may glide in direct touch with respect to others due to irreversible shear of thin films of the firmly adsorbed highly viscous water. These contacts are considered as not removable with a decrease of pressure [9].

In the (M-W-M) contacts the grains are separated by large cushions of loosely adsorbed water which deforms reversibly under loading, giving rise to global elastic strains. Plastic deformation of clay corresponds to an increase of the number of (M-M) contacts instead of (M-W-M) contacts. Heating reduces specific density and thus viscosity and stiffness of loosely adsorbed

water cushions. This facilitates formation of (M-M) contacts, and thus globally produces irreversible strains.

The above considerations are purely qualitative at the moment and call for systematic experimental and theoretical studies. They are not only of theoretical interest but would be utmost useful for adequate evaluation of the volume of expanded clay water and thus of the skeleton deformability.

11.3 THERMOMECHANICAL AND HYDRAULIC MATHEMATICAL MODEL FOR CLAYS

11.3.1 Thermo-elastoplastic model

From the macroscopic point of view two important conclusions may be drawn from the normal consolidation tests presented in previous sections. Firstly, since the effective stress is constant, the plastic volumetric strain hardening produced in heating is compensated by a 'temperature softening' corresponding to a yield surface shrinking. Secondly, no plastic strain increment is produced during cooling. Thus no strain hardening occurs. The temperature decreases however, and gives rise to a yield surface recovery (growth), while the stress point remains fixed in the interior of the elastic domain. Indeed, suppose that after cooling has been completed the mechanical loading continues. The stress path is first elastic until the expanded yield surface is reached, then elastoplastic yielding occurs, as seen from the post-cooling loading modulus in Figure 11.3a. The former observation, if considered from the point of view of plasticity theory, determines the form of the thermal dependence of the yield surface. In fact, take the consistency equation

$$df = \mathbf{f}_{,\sigma'}^T d\sigma' + f_{,a} \frac{\partial a}{\partial \epsilon_p} d\epsilon_p + f_{,T} dT = 0; \quad \frac{\partial f}{\partial x} \equiv f_{,x} \quad (11.5)$$

which must be satisfied during continuous yielding. Because the effective stress is kept constant during heating Equation (11.5) yields

$$f_{,T} = -\text{tr}(\mathbf{f}_{,\sigma'}) f_{,a} \frac{\partial a}{\partial \epsilon_p} \frac{d\lambda(dT)}{dT} \quad (11.6)$$

$$\sigma' = \text{const}$$

From the plastic work non-negativeness requirement $d\lambda$ is always positive at yielding; $\text{tr}(\mathbf{f}_{,\sigma'})$ is positive at isotropic stress state, while $(f_{,a} \partial a / \partial \epsilon_p)$ is negative by the definition of plastic hardening at constant temperature. Thus $f_{,T}$ must be positive. In the $\text{tr } \sigma', \mathbf{S}^T \mathbf{S}$ plane it means a yield surface regression with the temperature increase. The specific form of the thermal sensitivity of the yield surface is expressed through the function $a(\Delta T)$ taken as follows:

$$a = \frac{1}{2} \bar{a} \exp \left\{ \frac{1}{\lambda - K_i} [e_1 - e_g - e^{p/l} (1 - a_0 \Delta T)] \right\} + a_1 \Delta T + a_2 \Delta T^2 \quad (11.7)$$

where

K_i is the value of bulk modulus at $T = T_0$, $\bar{a} = 1 \text{ kg/cm}^2$
 e^{pl} is a hardening parameter expressed in terms of void ratio defined as

$$e^{pl} = (1 + e_0)\epsilon_0^p \quad (11.8)$$

e_1 void ratio at 1 kg/cm^2 and $\text{tr } \sigma'_g = 1 \text{ kg/cm}^2$

e_g is a fictitious plastic variation of the void ratio in a fictitious isotropic deformation between $e = e_1$ and the geostatic state $\sigma'_g, T = T_g$.

The plastic strain rate entity is ruled by the plastic multiplier $d\lambda$ which is determined from the consistency Equation (11.5) as

$$d\lambda = \frac{1}{\Delta H} (\mathbf{M}^T d\tilde{\mathbf{e}} + f_{,T} dT) \quad (11.9)$$

where $d\tilde{\mathbf{e}}$ is referred to as mechanically induced skeleton deformation defined as

$$d\tilde{\mathbf{e}} = d\mathbf{e} - \left(-\frac{1}{3}\tilde{\mathbf{C}}^* du + \tilde{\alpha}_T dT\right)\mathbf{m} \quad (11.10)$$

while $\tilde{\alpha}_T$ is an incremental coefficient of thermal expansion of the skeleton determined as a combination of α_{st} and $K(\Delta T)$ defined in Equation (11.1),

$$\tilde{\alpha}_T = -\frac{1}{1 + e_0} \frac{\partial K}{\partial T} \ln \frac{\text{tr } \sigma'}{\text{tr } \sigma'_g} + \alpha^* + \alpha_{st} + \frac{\partial \alpha_{st}}{\partial T} \Delta T \quad (11.11)$$

and $\tilde{\mathbf{C}}^*$ is an incremental grain/skeleton isotropic thermoelastic compliance ratio

$$\tilde{\mathbf{C}}^* = \frac{1}{3}\tilde{\mathbf{C}}^* \left[-\frac{K}{(1 + e_0)} + \frac{\partial \alpha_{st}}{\partial T} \Delta T \right]^{-1} \text{tr } \sigma' \quad (11.12)$$

The brittleness index ΔH , denoting by \mathbf{D}^{-1} the incremental thermoelastic matrix, is defined as

$$\Delta H = -f_{,e_0} \text{tr}(\mathbf{f}_{,\sigma'}) + \mathbf{f}_{,\sigma'}^T \mathbf{D}^{-1} \mathbf{g}_{,\sigma'}. \quad (11.13)$$

The brittleness index ΔH describes an incremental compliance (plastic strain-stress invariant curve slope). The behaviour becomes perfectly brittle when $\Delta H \rightarrow 0$, while it is perfectly plastic when $\text{tr}(\mathbf{f}_{,\sigma'}) = 0$. Finally the vector \mathbf{M} is defined as

$$\mathbf{M} = \mathbf{D}^{-1} \mathbf{f}_{,\sigma'}. \quad (11.14)$$

Having determined the plastic multiplier $d\lambda$ one may obtain an inverse strain-effective stress incremental relationship by combining an incremental form of the thermoplasticity relationship (11.9) and the consistency equation (11.5)

$$d\sigma' = \mathbf{D}^{ep} d\tilde{\mathbf{e}} + \mathbf{h} dT \quad (11.15)$$

where \mathbf{D}^{ep} is the thermo-elastoplastic stiffness matrix

$$\mathbf{D}^{ep} = \mathbf{D}^{-1} - \frac{1}{\Delta H} \mathbf{U} \mathbf{M}^T; \quad \mathbf{U} = \mathbf{D}^{-1} \mathbf{g}_{,\sigma'} \quad (11.16)$$

while \mathbf{h} is a thermal contribution stress vector standing for

$$\mathbf{h} = \frac{1}{\Delta H} f_{,T} \mathbf{U}. \quad (11.17)$$

Equation (11.15) has been formulated so that it does not differ from the form of the incremental stress-strain relationship for thermoplasticity of metals, see e.g. [11]. Note, however, that here the incremental strain $d\tilde{\mathbf{e}}$ encompasses contributions of $d\mathbf{e}$, dT and du . Moreover, the non-associativity of the flow rule, $\mathbf{U} \neq \mathbf{M}$, implies that the matrix \mathbf{D}^{ep} is non-symmetric. From preliminary results, not included in this paper, it appears that deviation of \mathbf{U} from \mathbf{M} becomes very significant mostly in the softening range, at higher temperatures.

Let us discuss now plastic loading and unloading conditions in the presence of temperature and water pressure. It is well known that a usual condition of unloading expressed in terms of the stress increment

$$d\lambda = 0, \quad \text{if } f < 0 \quad \text{or } f = 0 \quad \text{and } \mathbf{f}_{,\sigma'}^T d\sigma' + f_{,T} dT \leq 0 \quad (11.18)$$

fails to be unique when softening occurs (see e.g. [12]) i.e. when stress controllability does not hold. However, a standard procedure of expressing the inequality (11.18) in terms of the control parameter, i.e. $d\mathbf{e}$ may still be adopted. Substituting in the unloading condition, i.e. when the stress-strain law is elastic, the stress rate expressed through an incremental strain from equation (11.1) one obtains unloading condition and loading condition respectively at $f = 0$:

$$\mathbf{M}^T d\mathbf{e} + \mathbf{f}_{,\sigma'}^T \mathbf{m} \tilde{\mathbf{C}}^* du + (f_{,T} - \mathbf{f}_{,\sigma'}^T \mathbf{m} \alpha_T) dT \begin{cases} \leq 0; & \text{unloading} \\ > 0; & \text{loading} \end{cases} \quad (11.19)$$

where α_T stands for

$$\alpha_T = \tilde{\alpha}_T \text{tr } \sigma' \left(-\frac{K}{1 + e_0} + \frac{\partial \alpha_{st}}{\partial \ln(\text{tr } \sigma' / \text{tr } \sigma'_g)} \right)^{-1}. \quad (11.20)$$

The above system of equations and inequalities has been derived assuming that the temperature variation and the pore pressure build up are known *a priori*. However, this rarely happens both in laboratory homogeneous element simulation and in boundary value problems.

In general, temperature and pore pressure increments are unknown variables entering together with volumetric deformation a coupled partial differential equation system of mass flow continuity and of heat transport. The unloading condition (11.19) is therefore an *a posteriori* condition. Simplifying hypotheses are often made such as those on perfect drainage conditions for

which $u = 0$, or on perfect impermeability of the medium from which an additional condition is obtained allowing to eliminate u . Finally, the temperature field can be treated as independent from mechanical and hydraulic fields.

11.3.2 Transient flow in clay due to heating

The basic assumption for the flow of water through heated clay is that of water mass conservation

$$\frac{\partial(\rho^w n)}{\partial t} - \frac{\partial}{\partial x_i} (n \rho^w v_{si}) = 0 \tag{11.21}$$

in which ρ^w stands for the water specific density and n for the clay porosity, while v_{si} is an i th component of water flow velocity vector referred to a reduced area of effective channels in the soil. A global measure of the velocity per soil volume is $v_i = v_{si}/n$. Taking into account water density changes due to its deformability $\rho^w = \rho^{w0}(1 - \epsilon^w)$ and porosity changes due to clay deformation, the first term in (11.21) may be written

$$\frac{\partial(\rho^w n)}{\partial t} = -\rho^{w0} n \frac{\partial \epsilon^w}{\partial t} + \rho^{w0} \left(\frac{\partial \epsilon_v}{\partial t} - (1 - n) \frac{\partial \epsilon_v^*}{\partial t} \right) \tag{11.22}$$

where ρ^{w0} is an initial water density, ϵ^w is its volumetric strain, while ϵ_v^* is that of solid mineral of clay. Assuming that both ϵ^w and ϵ_v^* depend on water pressure and temperature and ϵ_v^* is sensitive to the effective isotropic stress equation (11.22) becomes

$$\begin{aligned} \frac{\partial(\rho^w n)}{\partial t} = & \rho^{w0} \left\{ n C^w(u, \Delta T) \frac{\partial u}{\partial t} - \left(\alpha^w + \frac{\partial \alpha^w}{\partial T} \Delta T \right) \frac{\partial T}{\partial t} \right. \\ & \left. + \frac{\partial \epsilon_v}{\partial t} + (1 - n) \left[\bar{C}^* \frac{\partial u}{\partial t} - \alpha^* \frac{\partial T}{\partial t} - \frac{1}{3} \frac{1}{1 - n} \bar{C}^* \frac{\partial \text{tr } \sigma'}{\partial t} \right] \right\}. \end{aligned} \tag{11.23}$$

Here C^w is the water compliance and α^w is its thermal expansion coefficient function, $\alpha^w = \alpha^w(\Delta T)$. The other term in the mass conservation equation (11.21) describing water flow through the soil is governed by a generalized Darcy law:

$$v_i = -k \frac{\partial}{\partial x_i} \left(\frac{u}{\rho^w g} + h \right) \tag{11.24}$$

where k is the permeability and $(u/(\rho^w g) + h)$ is the elevation head.

The permeability k is known to depend on the material porosity and water viscosity μ . The latter depends on temperature. Following Kézdi [13] the resultant permeability may be written as follows:

$$k = \frac{\gamma^w}{\mu_0} \frac{T - T^r}{K_0 S^2} \left(\frac{n}{1 - n} \right)^2 n \tag{11.25}$$

where μ_0 , K_0 , r are experimental coefficients, and S is specific surface area. Combining equations (11.23), (11.24), (11.25) and (11.21) one obtains finally a complete equation of mass conservation in terms of water pressure, strain temperature increments as follows

$$\begin{aligned} \frac{\partial}{\partial \mathbf{x}} \left(k \frac{\partial u}{\partial \mathbf{x}} \right) - \left(\mathbf{m}^T - \frac{1}{3} \bar{C}^* \mathbf{m}^T \mathbf{D}^{ep} \right) \frac{\partial \boldsymbol{\epsilon}}{\partial t} - \left(C^{**} - \frac{1}{9} \bar{C}^{**} \mathbf{m}^T \mathbf{D}^{ep} \mathbf{m} \right) \frac{\partial u}{\partial t} \\ - \left(\frac{1}{3} \bar{C}^* \mathbf{m}^T \mathbf{L}^{pl} + \alpha_v - \frac{1}{9} \bar{\alpha}_T \bar{C}^* \mathbf{m}^T \mathbf{D}^{ep} \mathbf{m} \right) \frac{\partial T}{\partial t} = 0 \end{aligned} \tag{11.26}$$

where

$$\begin{aligned} C^{**} = & (1 - n) \bar{C}^* + n C^w \\ \alpha_v = & n \alpha_w + (1 - n) \alpha^*. \end{aligned} \tag{11.27}$$

Rewriting the constitutive equation for the clay skeleton (11.15), taking into account the full form of the expression (11.10) referred to an infinitesimal time increment, the following system of equations is reached describing mechanical-hydraulic coupling at predetermined temperature increment

$$\begin{aligned} \begin{bmatrix} 0 & 0 \\ 0 & k \frac{\partial^2}{\partial \mathbf{x}} \end{bmatrix} \begin{Bmatrix} \boldsymbol{\epsilon} \\ u \end{Bmatrix} + \begin{bmatrix} \mathbf{D}^{ep} & \\ -\mathbf{m}^T + \frac{1}{3} \bar{C}^* \mathbf{m}^T \mathbf{D}^{ep} & -C^{**} + \frac{1}{9} \bar{C}^{**} \mathbf{m}^T \mathbf{D}^{ep} \mathbf{m} \end{bmatrix} \begin{Bmatrix} \dot{\boldsymbol{\epsilon}} \\ \dot{u} \end{Bmatrix} \\ + \begin{Bmatrix} -\frac{1}{3} \bar{\alpha}_T \mathbf{D}^{ep} \mathbf{m} + \mathbf{g}^{pl} \\ \frac{1}{3} \bar{C}^* \mathbf{m}^T \mathbf{L}^{pl} + \alpha_v - \frac{1}{9} \bar{\alpha}_T \bar{C}^* \mathbf{m}^T \mathbf{D}^{ep} \mathbf{m} \end{Bmatrix} \dot{T} = \begin{Bmatrix} \dot{\sigma}' \\ 0 \end{Bmatrix}. \end{aligned} \tag{11.28}$$

Clearly, this system is valid if elastoplastic loading condition is satisfied. If not, an incremental form of the constitutive equation (11.1) should be employed for $\partial \epsilon_v / \partial t$ in equation (11.26).

11.4 CLAY BEHAVIOUR DUE TO HEATING IN UNDRAINED CONDITIONS

For very short-term problems, like these of repository construction and canister emplacement procedures, undrained conditions are expected to simulate well clay behaviour mostly because of the extremely low permeability implying no flow at any point of the medium. Introducing the condition $K = 0$ in equation (11.24) a decoupling of mechanic the and hydraulic problem may be reached. Note first, that equation (11.26) becomes now

$$\frac{\partial \epsilon_v}{\partial t} + C^{**} \frac{\partial u}{\partial t} - \alpha_v \frac{\partial T}{\partial t} - \frac{1}{3} \bar{C}^* \frac{\partial \text{tr } \sigma'}{\partial t}. \tag{11.29}$$

An essential simplification may be obtained by substituting in equations (11.29) and (11.15) the pore pressure increment without involving now the fluid velocity equation. To reach such a goal the undrained condition equation must be introduced also in the equation for the plastic flow.

Thus a decoupled system is reached in which

$$d\boldsymbol{\sigma} = (\mathbf{D}^{ep} + \mathbf{C}^{pu}\mathbf{RR}^T) d\boldsymbol{\varepsilon} + \left(\mathbf{Q}^\alpha - \frac{1}{\Delta H} f, T\mathbf{M} \right) dT \quad (11.30)$$

$$du = C^{pu}\mathbf{R}^T d\boldsymbol{\varepsilon} + \left(\alpha_q + \frac{1}{C^*} \alpha_T \right) dT \quad (11.31)$$

where

$$\mathbf{R} = \left(\frac{1}{3} \bar{C}^* \mathbf{D}^{ep} - \mathbf{I} \right) \mathbf{m}; \quad \mathbf{Q}^\alpha = \left(\frac{1}{3} \bar{C}^* \alpha_g \mathbf{D}^{ep} - \mathbf{I} \right) \mathbf{m} \quad (11.32)$$

$$\alpha_q = -\frac{\alpha_T}{C^*} + C^{pu} \left[\alpha_v - \frac{1}{9} \bar{C}^* \bar{\alpha}_T \mathbf{m}^T \mathbf{D}^{ep} \mathbf{m} - \frac{1}{3} C^* \mathbf{m}^T \bar{C}^* - \frac{f, T}{\Delta H} \right] \quad (11.33)$$

$$C^{pu} = [C^{**} - \left(\frac{1}{3} \bar{C}^* \right)^2 \mathbf{m}^T \mathbf{D}^{ep} \mathbf{m}]^{-1}. \quad (11.34)$$

As for the transient flow case, the temperature is considered here as an independent variable.

Also the condition of unloading may be expressed explicitly getting rid of the pore pressure increment through (11.29). Thus $d\hat{\lambda} = 0$, if

$$f < 0 \quad \text{or} \quad f = 0, \quad \tilde{\mathbf{M}}^T d\boldsymbol{\varepsilon} + (f, T - \mathbf{f}_{, \sigma'}^T \mathbf{m} \alpha_T + \alpha_c) dT \leq 0 \quad (11.35)$$

where

$$\tilde{\mathbf{M}} = \tilde{\mathbf{D}}^{-1} \mathbf{f}_{, \sigma'}, \quad \alpha_c = \frac{(3\alpha_T/b_d) + \alpha_v(\bar{C}^*/C^{**})}{\frac{1}{\bar{C}^{**2}} - \frac{B_d}{C^{**}}} \quad (11.36)$$

The matrix $\tilde{\mathbf{D}}^{-1}$ is made of the matrix \mathbf{D}^{-1} by substituting B_d with

$$\tilde{B}_d = B_d \frac{3C^{**} - \bar{C}^*}{3C^{**} - \bar{C}^{**2} B_d} \quad (11.37)$$

where

$$B_d = \left(-\frac{K(\Delta T)}{1 + l_0} + \frac{\partial \alpha_{st}}{\partial T} \Delta T \right)^{-1} \text{tr } \boldsymbol{\sigma}' \quad (11.38)$$

Therefore, the unloading condition (11.18) becomes again an *a priori* condition provided dT is known.

11.5 HEAT TRANSPORT THROUGH CLAY

The heat transport through clay formation is potentially affected by the seepage of pore water and by soil porosity changes due to mechanical loads.

The transport equation in general reads:

$$\frac{\partial}{\partial \mathbf{x}} \left(\lambda \frac{\partial T}{\partial \mathbf{x}} \right) = \rho^w c^w \mathbf{v}^T \frac{\partial T}{\partial \mathbf{x}} + \frac{\partial}{\partial t} (\rho c \Delta T)_v \quad (11.39)$$

where λ is thermal conductivity of soil, $\rho^w c^w$ and ρc are specific heat capacities of water and of soil. Assuming that clay is fully saturated and that water and solid densities are constant

$$\rho = n\rho^w + (1 - n)\rho^*, \quad d\rho = c \Delta T(\rho^w - \rho^*) dn \quad (11.40)$$

one may obtain the following equation

$$\frac{\partial}{\partial \mathbf{x}} \left(\lambda \frac{\partial T}{\partial \mathbf{x}} \right) = \rho c \frac{\partial T}{\partial t} + \rho^w c^w \mathbf{v}^T \frac{\partial T}{\partial \mathbf{x}} + c \Delta T(\rho^w - \rho^*) \frac{dn}{dt}. \quad (11.41)$$

The second term of the rhs of (11.41) represents coupling of the thermal problem with the hydraulic one, whereas the third term is coupled with the mechanical one.

Preliminary results on Boom clay show that the coefficient of thermal conductivity increases with temperature, and similarly does the specific heat [14]. These data require anyway a larger experimental confirmation.

11.6 FINITE ELEMENT APPROXIMATION

Finite element approximation of the solution of boundary value problems governed by the previously presented equations has been undertaken under the main hypothesis of decoupling of the heat transfer equation. Physically it means that we neglect effects of heat transfers due to pore water flow and that we assume no variation of thermal properties of clay due to deformation. Thus the temperature field may be calculated using numerical techniques, as finite differences or finite elements, and considered to be known *a priori*, when a thermally dependent mechanical-hydraulic problem is approached. The attention here is therefore concentrated on the latter problem.

Note first, that in the case of undrained conditions, the water pressure variable is expressed through equation (11.31) and thus may be directly calculated if strain and stress are known. Therefore the numerical procedure is similar to that in a one-phase thermo-plasticity. The elemental equilibrium expressed in terms of element nodal force \mathbf{I} and external force \mathbf{E} vectors defined via usual interpolation function \mathbf{N} of surface traction t and body force \mathbf{b} vectors and congruence matrix \mathbf{B}

$$\mathbf{I} = \int_v \mathbf{B}^T \boldsymbol{\sigma} dv; \quad \mathbf{E} = \int_\Gamma \mathbf{N}^T t d\Gamma + \int_v \mathbf{N}^T \mathbf{b} dv \quad (11.42)$$

is found applying an algorithm based on Taylor expansion in series both of the variable \mathbf{I} , which is a non-linear function of the nodal displacements $\boldsymbol{\delta}$ and

of the nodal displacements themselves leading to the following system

$$\begin{aligned} \mathbf{z}_{i+1} &= (\mathbf{I}(\delta_i) - \mathbf{E})(\partial\mathbf{I}/\partial\delta)^{-1} \\ \delta_{i+1} &= \delta_i + \mathbf{z}_{i+1} \end{aligned} \quad (11.43)$$

where \mathbf{z}_{i+1} is an $(i + 1)$ -st correction to the displacement. The Jacobian $\partial\mathbf{I}/\partial\delta$ is obtained as a sum of the elemental matrices $J_e = \int (\mathbf{B}^T \partial\sigma/\partial\epsilon\mathbf{B}) dv_e$, which, result from the first term of the constitutive incremental stress-strain law for the undrained case, i.e.

$$d\sigma = (\mathbf{D}^{ep} + C^{pu}\mathbf{R}\mathbf{R}^T) d\epsilon. \quad (11.44)$$

The integration of the constitutive law is performed at imposed increments of strain and temperature at any Gauss point. First, it must be determined whether thermoelastic or thermoelastoplastic stress increment is activated. For the elastic strain, the deviatoric component law is linear, while the isotropic logarithmic law leads to a transcendental equation which is solved by the Newton method.

Consideration of the thermoelastoplastic path requires a determination of a possible elastic response part of a stress increment, i.e. of an intersection of the stress increment with the yield locus. Such an intersection is determined again by means of the Newton method expanding the yield surface in series with respect to both stress and temperature.

An integration of the thermoelastoplastic path proceeds by a subincrementation, which is chosen such as to guarantee the process accuracy. The plastic strain over the strain subincrement is calculated on the basis of intermediate values of yield surface gradients and hardening parameter. This procedure implies the application of an iterative scheme and the radial return rule. Then the remaining elastic strain increment is found and new stress point is obtained.

Also in the case of coupled seepage and deformation boundary value problem the Newton method has been adopted in order to solve the system of governing equations. It requires, however, their expansion with respect to both nodal displacements and nodal pore pressure variables.

Before however, the flow continuity equation has to be integrated with respect to time by a finite difference backward Euler method. The left-hand side of equation (11.26) is thus integrated for a finite time step Δt

$$\frac{\partial}{\partial \mathbf{x}} \left(\mathbf{K} \frac{\partial u}{\partial \mathbf{x}} \right) \Big|_{t=t_i} \Delta t$$

Taking the time integrated lhs of equation (11.26) integrated over the volume, and making use of the Gauss theorem for the above expression, both multiplied by a virtual pore pressure \tilde{u} one obtains the continuity equation

$$\int \Delta t \left[\tilde{u} (\Delta \epsilon_v + C^{**} \Delta u + \bar{C}^* \Delta(\text{tr } \sigma) - \alpha_v \Delta T) + \frac{\partial \tilde{u}}{\partial \mathbf{x}} \mathbf{K} \frac{\partial u}{\partial \mathbf{x}} \right] dv + \int_{\Gamma} \Delta t \tilde{u} \quad (11.45)$$

where \mathbf{v}_w is a boundary flow velocity and \mathbf{n} is the normal unit vector at the boundary. According to the backward difference procedure the variables are evaluated at the end of the step. Expanding now in series according to Newton method, the left-hand side of the continuity equation (11.45) with respect both to pore water pressure and displacement and analogously the equilibrium equation, the coupled system (11.28) takes on the following form

$$\int_V \left\{ -\tilde{u} \left(\mathbf{I} - \frac{1}{3} \bar{\mathbf{C}}^* \mathbf{D}^{ep} \mathbf{T} \right) \partial \epsilon - \tilde{u} \left(C^{**} - \frac{1}{9} C^{**2} \mathbf{ID}^{ep} \mathbf{I} \right) \partial u \right\} dv = A \quad (11.46)$$

where

$$A = \int_V \tilde{\epsilon}^T \sigma dv - \tilde{w} E$$

$$G = \Delta t \int_V \tilde{u} \mathbf{n}^T v_w d\Gamma + \int_V \left(\Delta t \frac{\partial \tilde{u}}{\partial \mathbf{x}} \mathbf{K} \frac{\partial u}{\partial \mathbf{x}} + \tilde{u} \{ \Delta \epsilon_v + C^{**} \Delta u + C^* \Delta \text{tr } \sigma' - \alpha_v \Delta T \right) dv.$$

By discretization via finite elements and by introducing nodal variables one finally obtain the coupled system for any virtual field of nodal pore pressure and nodal displacement variables as follows:

$$\begin{cases} \mathbf{C}_\delta \\ \mathbf{C}_u \end{cases} = \begin{bmatrix} \mathbf{K}_{11} & \mathbf{K}_{21}^T \\ \mathbf{K}_{21} & \mathbf{K}_{22} \end{bmatrix}^{-1} \begin{cases} \mathbf{F}_1 \\ \mathbf{F}_2 \end{cases}; \quad (11.47)$$

where \mathbf{C}_δ and \mathbf{C}_u are Newton corrections for displacements and pressures defined as

$$\begin{cases} \delta \\ \mathbf{u} \end{cases}_{i+1} = \begin{cases} \delta \\ \mathbf{u} \end{cases}_i + \begin{cases} \mathbf{C}_\delta \\ \mathbf{C}_u \end{cases}_{i+1} \quad (11.48)$$

while residual nodal force vector \mathbf{F}_1 and residual body force vector \mathbf{F}_2 read

$$\begin{aligned} \mathbf{F}_1 &= \int_V \mathbf{B}^T \sigma dv + \mathbf{E} \\ \mathbf{F}_2 &= \Delta t \left(\int_{\Gamma} \mathbf{N} \mathbf{q} d\Gamma + \int_V \mathbf{P}^T \mathbf{K} \mathbf{P} dv \cdot \mathbf{u} + \int_V \tilde{\mathbf{M}}^T \mathbf{m}^T \mathbf{B} dv (\delta_i - \delta_0) \right) \\ &\quad + \int_V \tilde{\mathbf{M}}^T C^{**} \tilde{\mathbf{M}} dv (\mathbf{u}_i - \mathbf{u}_0) + \int_V C^* \tilde{\mathbf{M}}^T \mathbf{m} (\sigma_i' - \sigma_0) dv \\ &\quad - \int_V \tilde{\mathbf{M}}^T \alpha_v \tilde{\mathbf{M}} dv (T_1 - T_0) \end{aligned} \quad (11.49)$$

where

$$\mathbf{P} = -\frac{\partial}{\partial \mathbf{x}} \bar{\mathbf{M}}.$$

The matrices $K_{21}^T = K_{12}$, K_{11} and K_{22} are respectively

$$K_{11} = \int_v \mathbf{B}^T \mathbf{D}^{ep} \mathbf{B} \, dv$$

$$K_{22} = \int_v \bar{\mathbf{M}}^T h \bar{\mathbf{M}} \, dv; \quad h = C^{**} - \frac{1}{9} C^{*2} \mathbf{ID}^{ep} \mathbf{I} \quad (11.50)$$

$$K_{12} = \int_v \mathbf{B}^T \mathbf{Z} \bar{\mathbf{M}} \, dv$$

with \mathbf{Z} denoting a collecting vector of all nodal values of elements of the matrix $\mathbf{I} - \frac{1}{3} \bar{C}^* \mathbf{D}^{ep} \mathbf{I}$ and $\bar{\mathbf{M}}$ standing for unit matrix.

The above described algorithm is implemented as a subroutine called CC-TER-U in options 'Transient flow' and 'Undrained' in a general purpose finite element computer code operating at ISMES.

11.7 A NEAR FIELD ANALYSIS

A simple case of a near field analysis has been undertaken using the above described mathematical model in order to design a medium scale laboratory experiment.

First an experiment on a small Pontida silty clay sample has been performed by heating the sample up to 92°C in undrained conditions. Figure 11.4(a) shows the stress path composed of an undrained shear loading up to conditions simulating a normally anisotropically consolidated clay state. After having allowed the material to creep till stabilization, heating has been performed under constant total stress. Correction for the water expansion contained in the apparatus, porous stones and tubes has been applied. As the result a net pore water pressure development in the specimen has been obtained as a function of the specimen vertical deformation, Figure 11.4(b). Failure has been reached at 92°C, and has been accompanied by a slight reduction of the pore which then stabilized. No localized shear band has been observed in this test. It was present in an analogous test performed on undisturbed Boom Clay sample, which however, is known to exhibit highly anisotropic behaviour. The stress path may be interpreted as partly elastic, what has been confirmed in a similar test with local unloadings. In the final phase however, the thermally reduced yield surface is reached. Then the yield surface shrinks at yielding, the effective isotropic stress decreases again a little and thus the pore pressure increases until the critical state is reached and plastic skeleton residual yielding is activated.

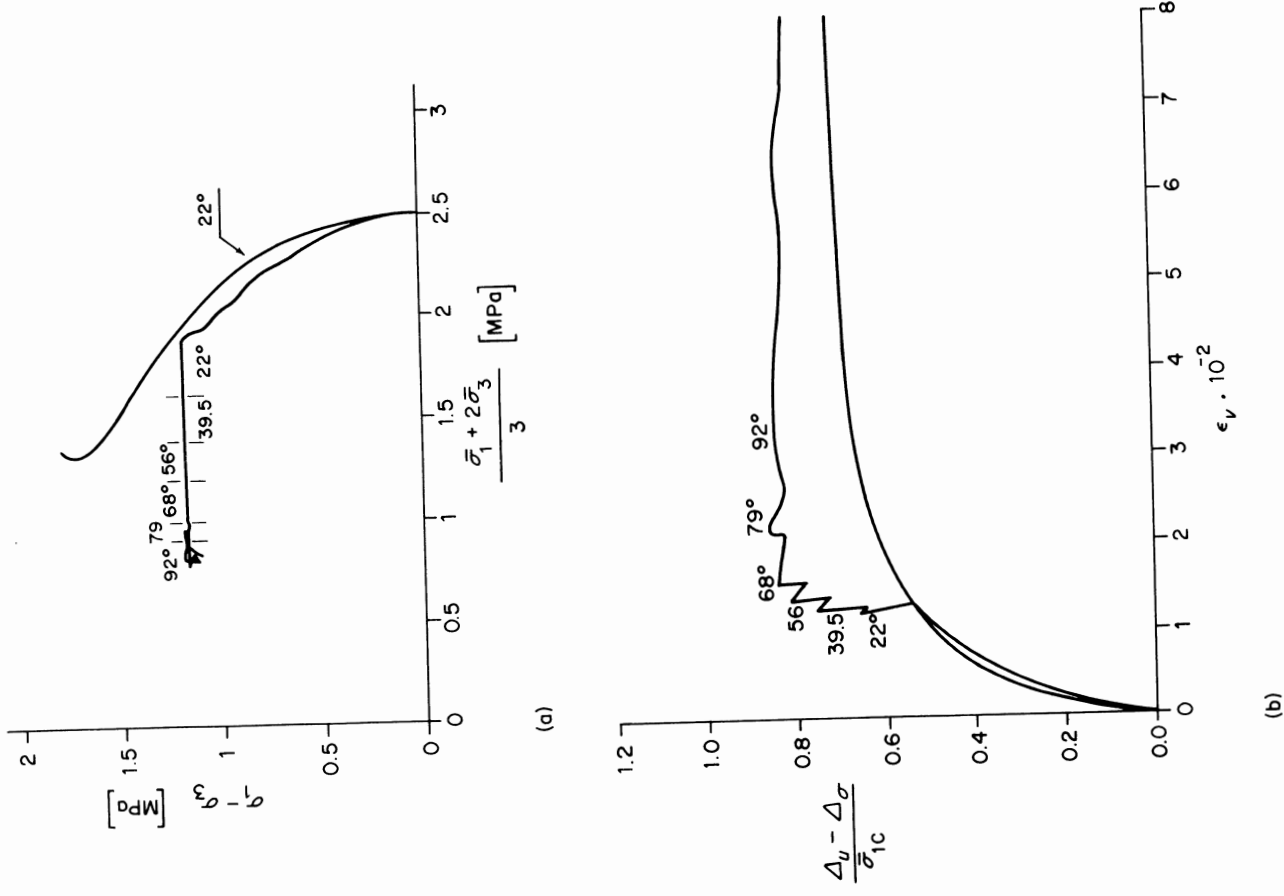


Figure 11.4 Undrained, constant deviator stress heating test on Pontida silty clay. (a) Effective stress path. (b) Vertical strain vs. water pressure.

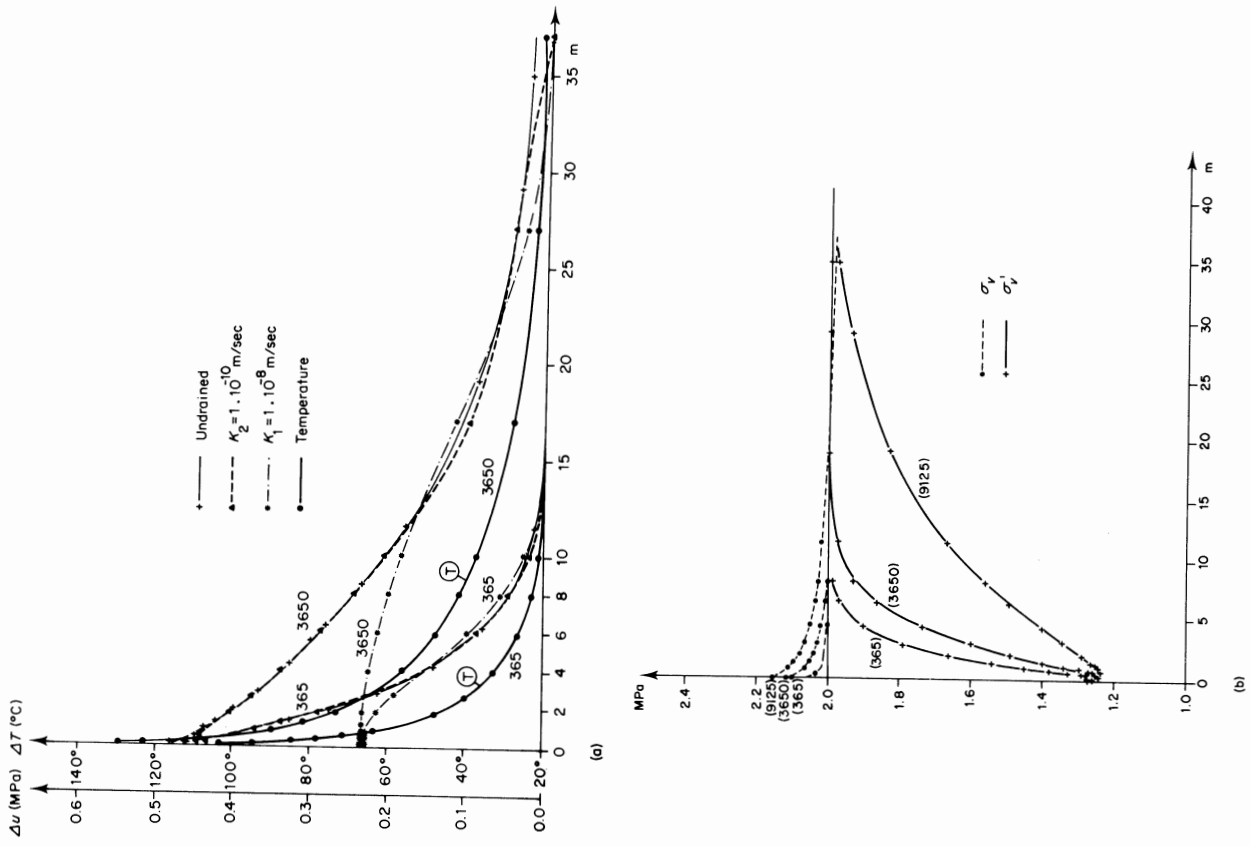
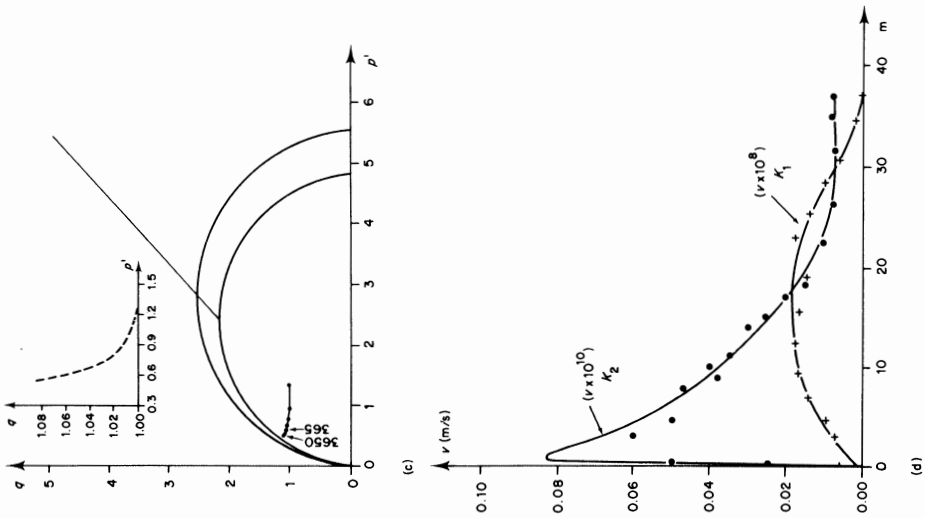


Figure 11.5 Numerical simulation of Pontida silty clay deposit response to central heating. (a) temperature and pore pressure distribution around the heater. (b) Total and effective vertical stress distribution. (c) Effective stress path. (d) Water flow radial velocity distribution at 10 years after emplacement.



The medium scale experiment has been simulated by the described model in the following way. The behaviour of an axisymmetrical Pontida silty clay column 90 m high and 37 m in radius has been simulated in plane strain. The column has been heated by a centrally placed heater of 15 cm radius emitting 224 W/m constant in time. The heater simulates a series of alternating HLW and CH containers 1.5 m high, emplaced 30 years after disposal from the reactor.

Figure 11.5(a) presents the distribution in the radial direction of temperature and excess pore pressure developed after one year and after ten years from the beginning of heating, for three cases of clay permeability, $K_1 = 1 \times 10^{-8}$ m/sec, $K_2 = 1 \times 10^{-10}$ m/sec and $K_3 = 0$. The first two cases have been studied with the 'Transient flow' option, while the latter with the option 'Undrained'.

Note first that the distribution of the pore pressure for $K_2 = 1 \times 10^{-10}$ m/sec. is almost identical to the 'undrained' solution both in the 1-year and in the 10-year analysis. Secondly, in the central, most heated zone the pressure is almost double for K_1 with respect to K_2 . At greater distances the difference diminishes. The vertical effective and total stress distributions, as well as flow velocities (Figure 11.5b, d) show quite significant effects in the range of about 18 m.

In Figure 11.5(c) the effective stress path is shown for the element closest to the heater, in analogy with the test result from the Figure 11.4(a). Although the stress does not reach the failure envelope, it markedly approaches it. Further post-yielding behaviour would involve both thermal and strain softening till the critical state is attained. In a homogeneous specimen the softening is an unstable process in terms of the second order work criterion [11]. As far as the evaluation of the overall stability of an undrained clay mass is concerned, further studies are required. In situ, there are undoubtedly several stabilizing effects and constraints like absence of initial pore pressure and contribution of stable adjacent zones (less heated and under different stress states). Anyhow, the destabilizing effects being localized, an overall stable situation is to be expected, see e.g. [15].

The above results indicate a relevance of heat induced variations of the original hydrological and mechanical conditions of clay formation in the near field. The far field water migration on geological scale seems to not be affected by the discussed phenomena. It means that mostly the engineering aspects of the thermally induced non-linear mechanical behaviour of clay have to be taken into account during repository design. To avoid adverse effects of water pressure build up an appropriate spacing of the canisters might be adopted. A possibility also arise to exploit beneficial effects of pore pressure excess such as improved self sealing due to enhanced plastic behaviour and facilitation of emplacement operations due to reduced shear resistance by heating.

11.8 CONCLUSIONS

In the paper non-linear thermal, coupled, hydraulic and mechanical properties of clays have been presented and a mathematical model has been described. The model has been formulated on the basis of preliminary experimental data. Systematic laboratory studies are now in progress guided by the above theory. Note, that some traditional simplifications of soil mechanics should be renounced and modifications were necessary in existing software to allow implementation of the model. It may be seen, for example, that water and soil compressibilities have to be taken into account for undrained conditions, due to pronounced thermal expansion of water. A complex behaviour of clay mass developing a remarkable pore water pressure under constant external force system due to heating was simulated.

ACKNOWLEDGEMENT

This work has been carried out at ISMES as a part of a research programme supported by ENEL (National Board of Electricity), ENEA (National Board for Alternative Energies of Italy) and by the Commission of European Communities.

REFERENCES

1. Heremans, R. Experimentation, and evaluation of near field phenomena in clay: the Belgian approach. in *Near-field Phenomena in Geologic Repositories for Nuclear Waste*, Proc. of Workshop, Seattle, Wa, OECD/NEA, Paris, 1981.
2. Borsetto, M., Cricchi, D., Hueckel, T., and Peano, A. On numerical models for the analysis of nuclear waste disposal in geologic clay formations. In *Numerical Methods for Transient and Coupled Problems*, (R. W. Lewis, et al. eds), Pineridge Press, Swansea U.K., 1984, pp. 608-618.
3. Campanella, R. G., and Mitchell, J. K. Influence of temperature variations on soil behaviour, *J. ASCE*, SM3, 709-734, 1968.
4. Baldi, G., Borsetto, M., Hueckel, T., and Tassoni, E., Thermally induced strains and pore pressures in clays. Submitted to Int. Symposium on Environmental Geotechnology, Allentown, 1985.
5. Heuzé, F. E. High temperature, mechanical, physical and thermal properties of granitic rocks - a review. *Int. J. Rock Mechanics, Min. Sci.*, 20(1), 3-10, 1983.
6. Roscoe, R., and Burland, J. In *Engineering Plasticity* J. Heyman, and F. A. Leckie (ed), Cambridge University Press, 1968, p. 35.
7. Gudehus, G. Elastoplastische Stoffgleichungen für trockenen Sand, *Ing. Arch.*, 42, 583-599, 1973.
8. Grim, R. E. *Applied Clay Mineralogy*, McGraw Hill, N.Y. 1962, p. 422.
9. Rosenquist, T. Physico-chemical properties of soils soil-water system, *Proc. ASCE*, SM2, 31-53, 1959.
10. Resendiz, D., On the strength of clayey soils, Univ. Nac. Aut. de Mexico, 1965.
11. Prager, W. Non-isothermal plastic deformation, *Proc. K. Nederl. Academie van Wetenschappen B.61/3*, 176-182, 1958.
12. Maier, G., and Hueckel, T. Non-associated and coupled flow rules of elastoplasticity for rock-like materials, *Int. J. Rock Mechanics and Mining Sciences*, 16, 77-92, 1979.
13. Kézdi, A. *Handbook of Soil Mechanics*, Vol. 1 *Soil Physics*, Elsevier, Amsterdam, 1979.
14. Heremans, R., Bingsens, M., and Manfroy P. Le comportement de l'argille vis-à-vis de la chaleur, Proc. *In Situ Heating Experiments in Geologic Formations*, Ludvika/Stripa, 1978.
15. Hueckel, T., and Maier G. Incremental boundary value problems in presence of coupling of elastic and plastic deformation; a rock mechanics oriented theory, *Int. J. Solids and Structures*, 13(1), 1-15, 1977.